Available online at www.sciencedirect.com
SCIENCE DIRECT
Polymer 47 (2006) 1357–1363
polymer
www.elsevier.com/locate/polymer

Effect of crystallinity and loading-rate on mode I fracture behavior of poly(lactic acid)

Sang Dae Park [a], Mitsugu Todo [a,*], Kazuo Arakawa [a], Masaaki Koganemaru [b]

[a] *Research Institute for Applied Mechanics, Kyushu University, Kasuga, Fukuoka 816-8580, Japan*
[b] *Mechanics and Electronics Research Institute, Fukuoka Industrial Technology Center, Kitakyushu, Fukuoka 807-0831, Japan*

Received 4 April 2005; received in revised form 14 October 2005; accepted 11 December 2005
Available online 10 January 2006

Abstract

The aim of this study is to characterize the fracture behavior of biodegradable poly(lactic acid) (PLA). Especially, the effects of crystallinity and loading-rate on the fracture behavior are emphasized. Annealing was performed to control the crystallinity of the PLA samples prepared, and then their fracture toughness values were measured under quasi-static and impact loading conditions. The results showed that the quasi-static fracture toughness of PLA decreases with increase of crystallinity; on the other hand, the impact fracture toughness tends to increase with crystallinity. The crack growth behaviors of the PLA specimens having different crystallinity were also observed by polarizing and scanning electron microscopies. The microscopic results exhibited that under quasi-static loading, disappearance of multiple crazes in the crack-tip region results in the decrease of the fracture toughness with crystallinity. On the contrary, under impact loading, the increase of the fracture toughness with crystallinity is considered to be related to the increase of fibril formation.

Keywords: Biodegradable polymer; Fracture toughness; Crystallinity

1. Introduction

Poly(lactic acid) (PLA), a biodegradable polymer, has widely been used in industrial applications such as interior parts of automobiles, exterior parts of electric devices and food packages. Recently, PLA is also considered to be used as a biomaterial mainly due to its bioabsorbability and biocompatibility. For example, it has been used for bone fixation devices in orthopedic and oral surgeries. Since bioabsorbability is one of the key factors for PLA medical devices, some of the studies have mainly focused on the degradation behavior in vivo and in vitro [1–5]. Some fundamental studies were also performed to characterize the crystallization behavior and mechanical properties of thin PLA films [6–9]. Although such PLA implants are in bulk forms such as plate, rod and screw, a few studies have been performed to characterize the mechanical behavior of PLA solids [10,11]. In addition, it is reported that fracture of PLA implants sometimes occurs in medical application, while the fracture behavior of PLA has not sufficiently been understood yet.

The aim of this study is to characterize the effects of crystallization and loading-rate on the mode I fracture toughness and mechanism of PLA. Annealing was performed to control the microstructure of the PLA samples. Microstructures were then observed using a polarizing microscope (POM). Thermal and dynamic mechanical properties were measured by a differential scanning calorimetry (DSC) and a dynamic mechanical analyser (DMA), respectively. Mode I fracture tests were performed to measure the critical strain energy release rate as a mode I fracture toughness under static and impact loading-rates. Crack growth behaviors and fracture surfaces were also observed using POM and a scanning electron microscope (SEM) to characterize the fracture mechanisms, and the macroscopic fracture toughness values were then correlated with the microscopic mechanisms.

2. Experimental

2.1. Material and specimen

PLA pellets (Lacty#9030) were supplied by Shimadzu Co., Ltd as test sample. The content of L-form and the weight average molecular weight are 95% and 140,000 g mol^{-1}, respectively. Thermal properties of the pellets such as the glass transition, the melting and the crystallization temperature are

* Corresponding author. Tel.: +81 92 583 7762; fax: +81 92 583 7763.
E-mail address: tohdoh@raim.kyushu-u.ac.jp (M. Todo).

0032-3861/$ - see front matter © 2005 Elsevier Ltd. All rights reserved.
doi:10.1016/j.polymer.2005.12.046

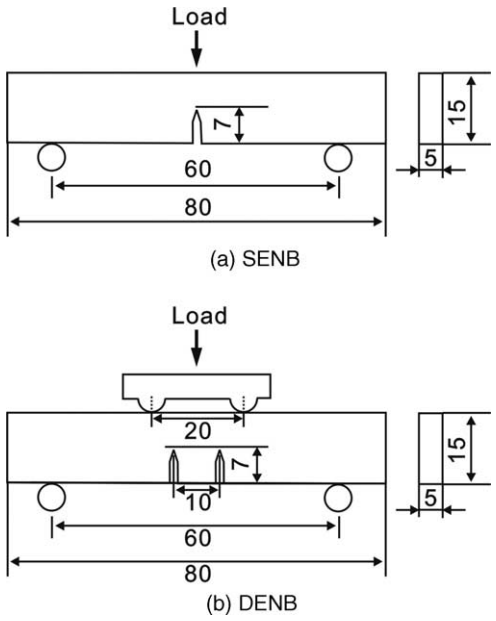

Fig. 1. Geometry of SENB and DENB specimens (unit, mm): (a) SENB; (b) DENB.

64, 167 and 123 °C, respectively. Plates of 5 mm thick were fabricated using a hot press installed with a water cooling system. Those Pellets were heated and melted at 180 °C, pressed for 30 min at 30 MPa and quenched for 10 min to room temperature. Some of the molded plates were then annealed in an oven under different conditions to obtain different microstructrues. The annealing temperatures chosen were 70 and 100 °C, and the holding times were 3, 8 and 24 h.

Single-edge-notch-bending (SENB) specimens were prepared from these PLA plates for mode I fracture toughness testing. Double-edge-notch-bending (DENB) specimens were also prepared for optical microscopy of crack growth behavior. The specimen geometries are shown in Fig. 1.

2.2. Measurement of crystallinity and spherulite size

Crystallinities of the PLA specimens fabricated were determined by DSC analysis using DSC-60 (Shimadzu Co., Ltd) equipped with a TA-60WS thermal analysis system. The apparatus was calibrated with an indium standard in nitrogen atmosphere. Samples of about 8–10 mg were placed in aluminum cells, and heated from 40 to 230 °C at a rate of 10 °C/min in nitrogen atmosphere. Crystallinity, X_c, was then evaluated using the following formula [8]:

$$X_C = \frac{100 \times (\Delta H_m + \Delta H_C)}{93} \quad (1)$$

where ΔH_m and ΔH_C are the enthalpies of melting and crystallization of the PLA samples, and 93 (J/g of polymer) is the enthalpy of fusion of PLA [12].

Thin films placed on slide glasses were prepared from the middle-sections of the PLA specimens using petrographic thin section technique. Spherulite structures of the thin films were observed using POM and photographed using a digital camera. For each of the specimens, the average size of spherulites was then measured from the digital image.

2.3. Dynamic mechanical analysis

Dynamic mechanical behaviors of the three PLA specimens with different microstructures, namely, an amorphous and two crystallized annealed under the conditions, 70 °C–24 h and 100 °C–24 h, were measured by DMA operated under tensile mode, using EXSTAR 6000 DMS (Seiko Instrument Inc.) at a frequency of 10 Hz and a heating rate of 2 °C/min in temperature range from 30 to 110 °C. Storage modulus, E', and loss tangent, $\tan\delta$, were obtained as a function of temperature, respectively.

2.4. Mode I fracture testing

Mode I fracture tests of the SENB specimens were performed at a loading-rate of 1 mm/min by a servohydraulic testing machine, and at an impact loading-rate of 1 m/s by an instrumented drop weight testing system with use of a dynamic displacement measuring apparatus [13]. The critical mode I energy release rate, G_{IC}, was then evaluated as the mode I fracture toughness using the following formula [14]:

$$G_{IC} = \frac{U_C}{BW\phi} \quad (2)$$

where U_c is the critical energy obtained as the area under the load-displacement curve which can be evaluated by numerically integrating the curve up to a critical point. In the present study, the critical point was chosen to be the maximum load point. B and W are the thickness and width of the specimen, respectively, and ϕ the geometrical correction factor given as a function of a/W where a is the initial crack length.

2.5. Polarizing and scanning electron microscopies

Thin section placed on slide glass was prepared using the petrographic thin section technique from each of the DENB samples tested in which one of two cracks was arrested and a process zone was developed in the crack-tip region [15]. Crack

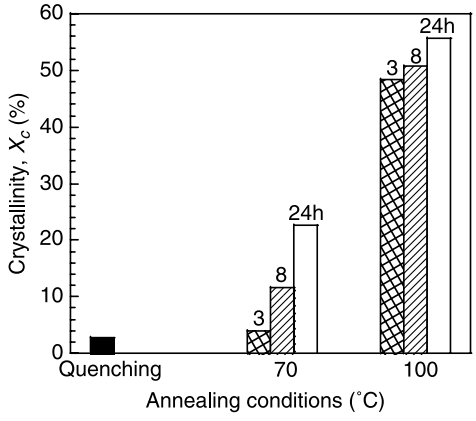

Fig. 2. Relationship between crystallinity and annealing condition.

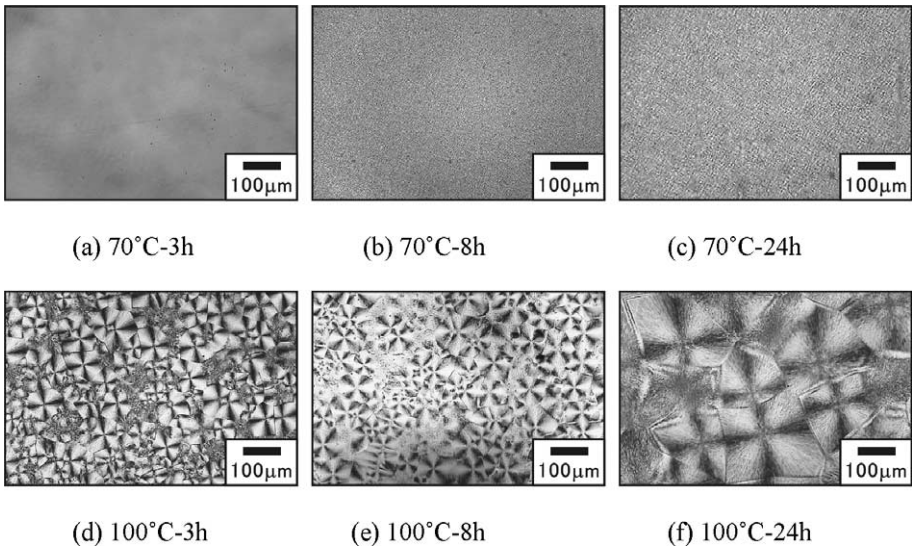

Fig. 3. Polarized micrographs of microstructures: (a) 70 °C–3 h; (b) 70 °C–8 h; (c) 70 °C–24 h; (d) 100 °C–3 h; (e) 100 °C–8 h; (f) 100 °C–24 h.

growth behavior was then characterized using POM. Fracture surfaces of the SENB specimens tested were also observed using SEM to study the effects of crystallization and loading-rate on the fracture surface morphology.

3. Results and discussion

3.1. Crystallinity and spherulite size

Effects of annealing conditions, temperature and time, on the crystallinity, X_c, evaluated using Eq. (1) are shown in Fig. 2. The lowest value of X_c is about 2.7% for the quenched sample, and X_c of the annealed samples increases with increase of annealing time and temperature. The highest X_c is about 56% for the 100 °C–24 h sample.

POM microphotographs of the microstructures are shown in Fig. 3. It is clearly observed that the density and size of spherulites increase with increase of annealing time and temperature. Relationship between the crystallinity and the spherulite size is shown in Fig. 4. It is clearly seen that the spherulite size increases with increase of crystallinity. The spherulite size linearly increases as X_c increases up to 48.3%, and rapidly increases above 48.3%. For a semi-crystalline polymer, in general, its crystal growth rate becomes faster when the annealing temperature is close to its crystallization temperature [16–18]. In the present study, the crystallization temperature of PLA is estimated as about 123 °C, and therefore, annealing at 100 °C results in faster crystal growth rate than annealing at 70 °C.

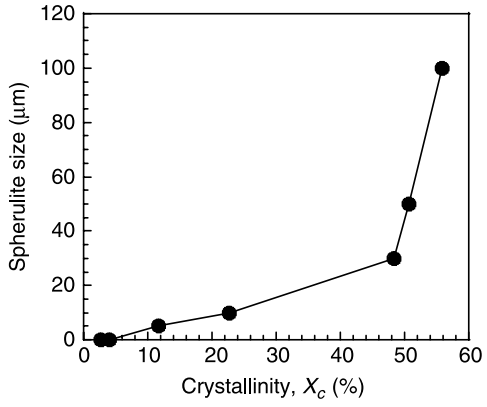

Fig. 4. Relationship between crystallinity and spherulite size.

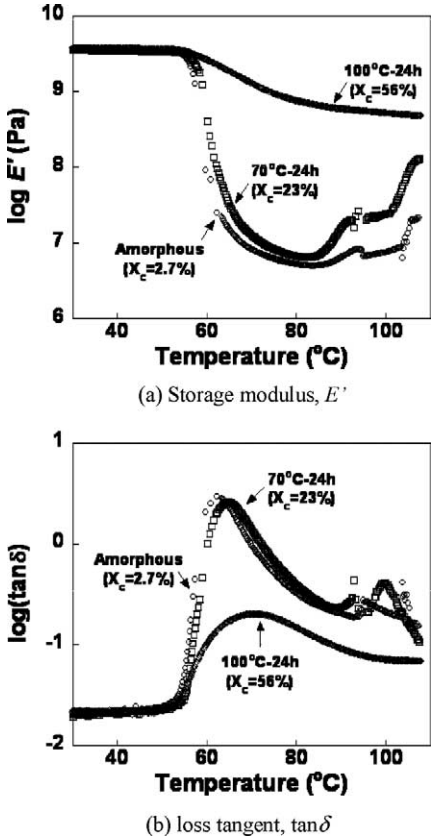

(a) Storage modulus, E'

(b) loss tangent, tanδ

Fig. 5. Dynamic mechanical spectrums as a function of temperature: (a) storage modulus, E'; (b) loss tangent, tan δ.

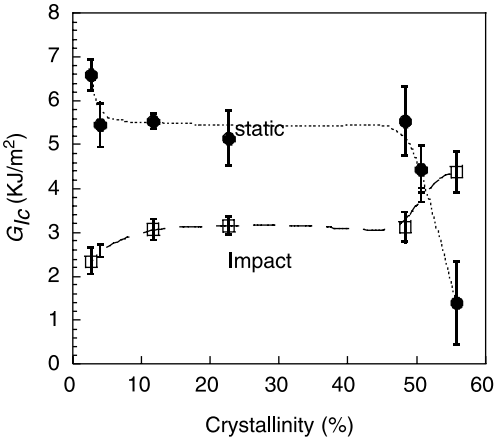

Fig. 6. Dependences of crystallinity on K_{IC} and G_{IC}.

3.2. Dynamic mechanical behaviors

E' and tan δ are shown as a function of temperature in Fig. 5. All three samples examined show sudden decreases of E' around 60 °C which is close to the glass transition temperature 64 °C of the pellets. The drop of E' values of the amorphous and the 70 °C–24 h samples is much faster than the highly crystallized 100 °C–24 h sample. Thus, annealing, therefore crystallization, can improve the heat resistance of PLA mainly due to the restraint of molecular motion by the formation of firm spherulites under the 100 °C–24 h condition. The sharp peaks of tan δ observed in Fig. 5(b) correspond to the glass transition temperature T_g, and the peak shifts to higher temperature with increase of crystallinity.

3.3. Critical stress intensity factor and energy release rate

Dependence of crystallinity on G_{IC} is shown in Fig. 6. At the quasi-static rate, G_{IC} slightly decreases with increase of

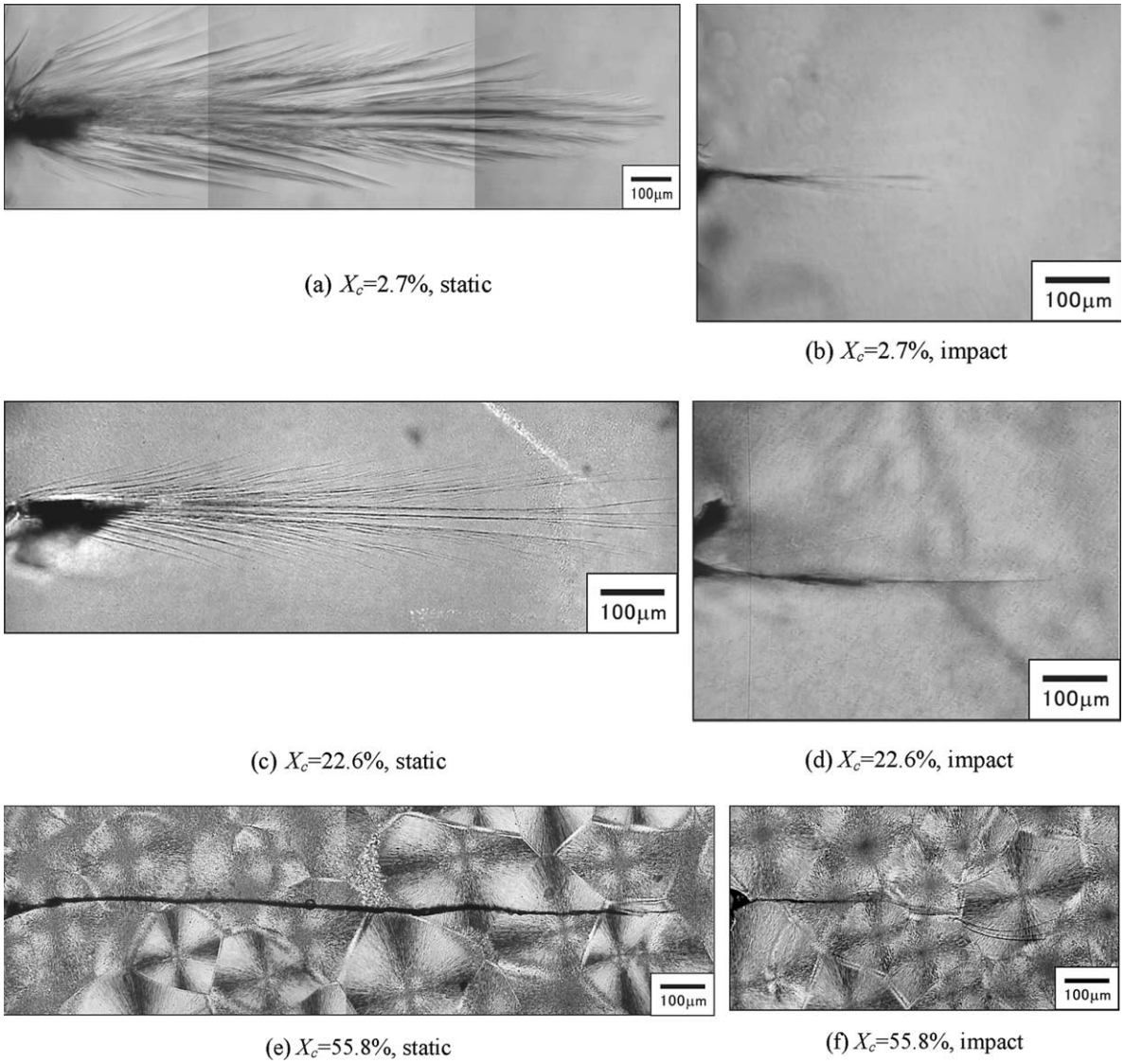

Fig. 7. Polarized micrographs of crack growth behaviors. (a) X_c = 2.7%, static; (b) X_c = 2.7%, impact; (c) X_c = 22.6%, static; (d) X_c = 22.6%, impact; (e) X_c = 55.8%, static; (f) X_c = 55.8%, impact.

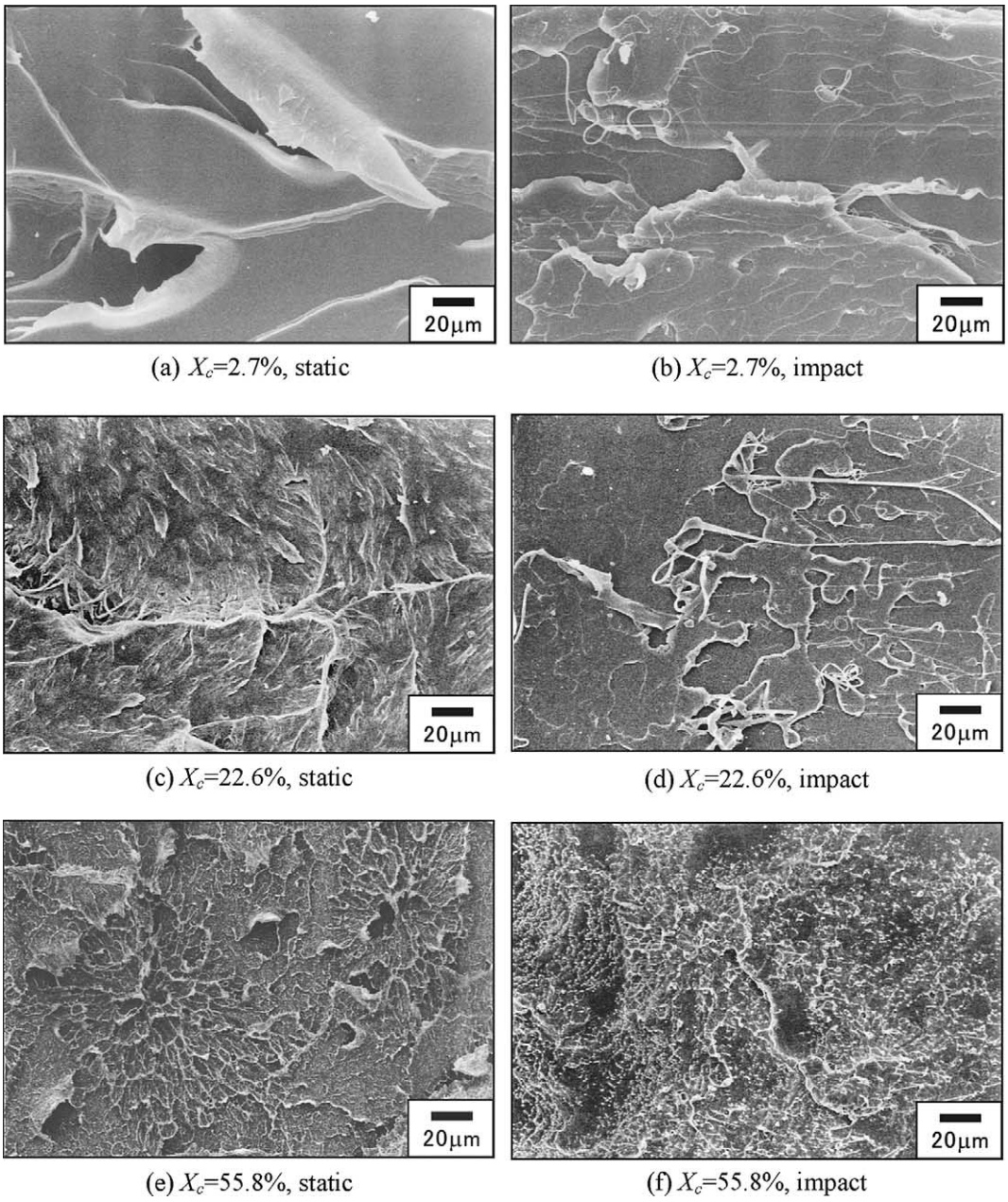

Fig. 8. SEM micrographs of fracture surfaces. (a) X_c=2.7%, static; (b) X_c=2.7%, impact; (c) X_c=22.6%, static; (d) X_c=22.6%, impact; (e) X_c=55.8%, static; (f) X_c=55.8%, impact.

crystallinity up to X_c=11.6, and kept constant up to X_c=48.3%. Above X_c=48.3%, G_{IC} rapidly decrease. It is well known that the fracture toughness of semi-crystalline polymers tends to decrease with increase of spherulite size [19], mainly due to increase of brittleness. It is, however, interesting to note that the elastic modulus [20] and the yield strength [17] tend to have a peak value at a moderate spherulite size.

On the other hand, at the impact rate, G_{IC} tends to increase with increase of crystallinity. As a result, the static G_{IC} is greater than the impact value up to X_c=48.3%, and above 48.3%, on the contrary, the impact value becomes higher than the static value. This result suggests that the fracture mechanism at the static rate is different from that at the impact rate.

3.4. Crack growth behaviors and fracture surface morphology

Fig. 7 shows polarized micrographs of arrested cracks in the PLA specimens prepared under different annealing conditions, and tested at both static and impact loading rates. For the amorphous specimen with X_c=2.7% under static loading (Fig. 7(a)), extensive multiple crazes were generated in the crack-tip region, while only a few crazes were observed under impact loading (Fig. 7(b)). This kind of craze formation in crack-tip region is usually observed in amorphous polymers such as polystyrene in which craze formation is dominant rather than shear plastic deformation [21]. For the samples with middle range of X_c (23%) (Fig. 7(c) and (d)), similar crack growth

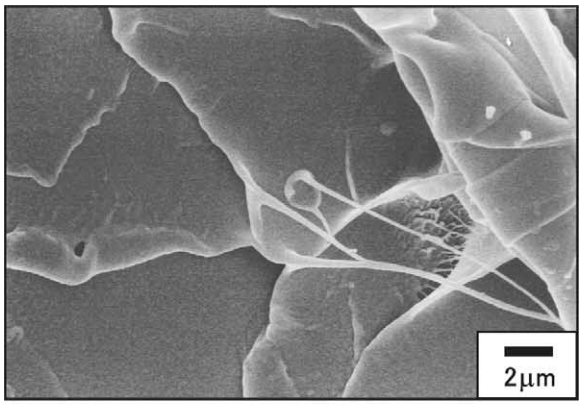

(a) X_c=2.7%

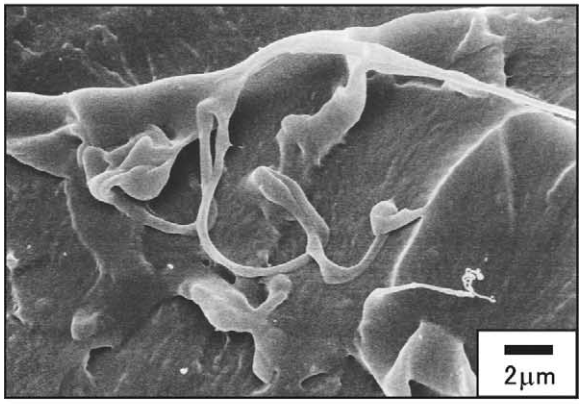

(b) X_c=22.6%

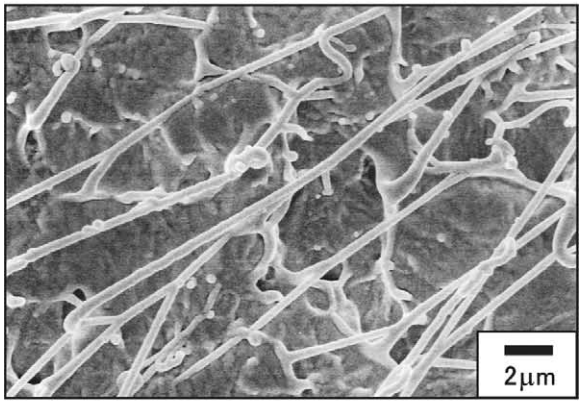

(c) X_c=55.8%

Fig. 9. Fibril structures appeared on the fracture surfaces under impact loading. (a) X_c=2.7%; (b) X_c=22.6%; (c) X_c=55.8%.

behaviors to the amorphous samples were observed under both static and impact loading. Disappearance of multiple craze formation observed at impact rate corresponds to the reduction of additional energy dissipation in the crack-tip region compared to the static case where multiple crazes are formed, and therefore results in the decrease of G_{IC} as shown in Fig. 6.

On the contrary, for the highly crystallized specimen with X_c=56% tested at static rate (Fig. 7(e)), a straight single crack without craze formation in the surroundings is observed. This type of crack growth usually corresponds to brittle fracture and lower G_{IC} than the amorphous dominant samples in which crazes are generated in crack-tip region. For crystalline polymers, two possible crack paths related to spherulite structure are considered: one is the inter-spherulitic crack growth, and the other the crack growth through spherulites. These crack paths related to crystal structure strongly depend on the formation process of the microstructure of the polymer [17,22]. Fig. 7(e) shows the crack mainly propagated through the spherulites, and therefore these spherulites were considered to be formed firmly each other. At impact rate (Fig. 7(f)), the main crack tends to be distorted and branched. These behaviors may be related to the increase of G_{IC} at impact rate, although the detail of the mechanism is still unclear, and further study will be performed to elucidate such mechanism.

Fig. 8 shows SEM micrographs of the fracture surfaces of the PLA samples. For the amorphous sample tested at the static rate (Fig. 8(a)), the fracture surface exhibits deep concavities and hackles due to multiple craze formation. The fracture surfaces of the crystallized samples (Fig. 8(c) and (e)) appears to be smoother than the amorphous one (Fig. 8(a)), corresponding to the decrease of the toughness values. The highly crystallized sample (Fig. 8(e)) also seems a bit smoother than the sample with lower crystallinity (Fig. 8(c)). The protrusions observed on the surfaces of the crystallized samples are considered to be composed of fibrils created by deformation of spherulites. The ultimate units composing these micro-fibrils are thought to be lamellar blocks of 10–20 nm thick [17,23].

The impact fracture surface of the amorphous sample (Fig. 8(b)) is obviously smoother than the static one (Fig. 8(a)), corresponding to the decrease of G_{IC}. It is noted that drawing fibrils are also observed on the impact fracture surface, suggesting that effect of high strain-rate exists. Roughness of the impact fracture surface appears to increase with increase of crystallinity comparing the surfaces shown in Fig. 8(b), (d) and (e). For the impact surface of the highly crystallized sample (Fig. 8(e)), relatively fine roughness exists suggesting the increase of G_{IC} as crystallinity increases. Ductile fibril formations are observed on all the impact surfaces as shown in Fig. 8. This kind of fibril formation appears to be related to increase of the temperature in the crack-tip region above the glass transition temperature due to heat generation at high strain-rate [24,25]. Fig. 9 also exhibits that the density of fibrils tends to increase as crystallinity increases, suggesting that the energy dissipation due to such ductile fibril formation also increases with crystallinity and therefore, G_{IC} increases.

4. Conclusions

PLA samples were annealed under several conditions to obtain different microstructures with varying spherulite size and density. Dynamic mechanical analysis was then performed to assess the effect of crystallization on dynamic viscoelastic properties. Mode I fracture testing of the PLA specimens was carried out to measure the critical strain energy release rate G_{IC}

as the mode I fracture toughness. Polarizing and scanning electron microscopies were also conducted to characterize the fracture mechanisms. The conclusions obtained are as follows:

(1) Heat resistance is dramatically improved as crystallinity. At quasi-static loading-rate, as crystallinity increased.
(2) The static values of G_{IC} decreased with increase of crystallinity due to disappearance of multiple craze formation, corresponding to decrease of amorphous region. On the contrary, at impact loading-rate, G_{IC} increased due to increase of fibril structure.
(3) For the amorphous PLA, the static toughness was higher than the impact one, mainly owing to extensive multiple craze formation at the static rate. On the contrary, for the crystallized PLA, the impact toughness became larger than the static one due to formation of fibril structure at the impact rate.

References

[1] Reed AM, Gilding DK. Polymer 1981;22:494.
[2] Li SM, Garreau H, Vent M. J Mater Sci, Mater Med 1990;1:123.
[3] Laitinen O, Törmälä P, Taurio R, Skutnabb K, Saarelainen K, Iivonen T, et al. Biomaterials 1992;13:1012.
[4] Hans P, Gutwald R, Ordung R, Reuther J, Mühling J. Biomaterials 1993; 14:671.
[5] Mainil-Varlet P, Rahn B, Gogolewski S. Biomaterials 1997;18:257.
[6] Kalb B, Pennings AJ. Polymer 1980;21:607.
[7] Hoogsteen W, Postema AR, Pennings AJ, Brinke G. Macromolecules 1990;23:634.
[8] Tsuji H, Ikada Y. Polymer 1995;36:2709.
[9] Miyata T, Masuko T. Polymer 1998;39:5515.
[10] Todo M, Shinohara N, Arakawa K. J Mater Sci Lett 2002;21:1203.
[11] Park SD, Todo M, Arakawa K. J Mater Sci 2004;39:1113.
[12] Fischer EW, Sterzel HJ, Wegner G. Kollid ZZ Polym 1973;251:980.
[13] Todo M, Nakamura T, Takahashi K. J Compos Mater 2000;34:630.
[14] ASTM D5045-91a.
[15] Sue HJ. Polym Eng Sci 1991;31:270.
[16] Keith HD, Padden FJ. J Appl Phys 1963;35:1286.
[17] Way JL, Atkinson JR, Nutting J. J Mater Sci 1974;9:293.
[18] Thomason JL, Van Rooyen AA. J Mater Sci 1992;27:889.
[19] Friedrich K. Advances in polymer science. Berlin: Springer; 1983 p. 225.
[20] Andrews EH. Pure Appl Chem 1974;39(1/2):179.
[21] Bosis J, Chudnovsky A, Moet A. Int J Frac 1987;33:263.
[22] Friedrich K. Proc ICF4 1977;3:1119.
[23] Andrews EH. J Polym Sci A-2 1966;4:668.
[24] Williams JG. Int J Frac Mech 1972;8:393.
[25] Fuller KNG, Fox PG, Field JE. Proc R Soc London 1975;A341:537.